Bull. Chem. Soc. Ethiop. **2024**, 38(1), 241-253.
DOI: https://dx.doi.org/10.4314/bcse.v38i1.18

ISSN 1011-3924
Printed in Ethiopia
Online ISSN 1726-801X

EVALUATION OF IMPROVED CORROSION RESISTANCE OF Zn ALLOY AS ELECTRODE MATERIAL BY Co_3O_4 COATINGS

R.J. Golden Renjith Nimal[1], D.F. Melvin Jose[2], K. Balasubramanian[3] and J. Sunil[4*]

[1]Department of Mechanical Engineering, Jai Shriram Engineering College, Avinashipalayam, Tirupur, Tamil Nadu, India
[2]Department of Mechanical Engineering, AL AZHAR College of Engineering & Technology, Thodupuzha, Idukki Dist. Kerala, India
[3]Department of Mechanical Engineering, Dr MGR Educational and Research Institute, Chennai, Tamil Nadu, India
[4]Department of Mechanical Engineering, Annai Vailankanni College of Engineering, Kanyakumari, Tamil Nadu, India

(Received August 7, 2023; Revised September 11, 2023; Accepted September 26, 2023)

ABSTRACT. This work uses the sonochemical method to represent synthesized cobalt oxide nanoparticles (Co_3O_4) and analysed using different techniques. The X-ray diffraction analysis (XRD) and Fourier-transform infrared spectroscopy (FTIR) examinations of the synthesized nanoparticles confirmed their cubic structure and average crystallite size of 21.3 nm. The spherical surface shape and presence of components with a particle size of 25.3 nm were revealed. Scanning probe microscopy (SPM) methods analysed the Co_3O_4 coated plates' surface characteristics, including roughness and topographical ideas. An aqueous electrolyte medium (6 M KOH) was used to investigate the electrochemical corrosion behaviour of Co_3O_4-coated plates. According to the Tafel plot, coating Zn plates with a high surface area and mesoporous Co_3O_4 in KOH electrolytes greatly reduced the corrosion of the plates. The coated plates are thermally treated up to 600°C. The temperature-dependent anticorrosive properties of Co_3O_4 NPs are evaluated.

KEY WORDS: Co_3O_4, Zn plate, Tafel plot, Linear sweep voltammetry, Anti-corrosive performance, Nanoindentation

INTRODUCTION

Electrochemical devices are critical in searching for renewable energy sources and innovative technological applications. Electrode materials are crucial to properly functioning electrochemical devices [1]. However, corrosion damage over time is a significant obstacle to their practical use since it decreases performance and shortens lifespans. To tackle this problem, researchers have been diligently looking for new methods to improve the electrode materials' resistance to corrosion. Material degradation due to interaction with its surrounding environment is known as corrosion. It's a big issue that threatens the efficiency and integrity of materials [2]. Loss of conductivity and performance due to erosion of electrodes might have adverse effects in particular instances. The presence of oxygen, moisture, and chemicals are all potential causes of corrosion.

The corrosion rate may be affected by several factors, including the material type and surface condition. Coatings, like paints and plastics, have traditionally been used for corrosion prevention. Corrosion might reoccur if these coatings wear out or get damaged [3]. Nanoparticles to improve materials' resistance to corrosion have gained popularity in recent years. A typical description of nanomaterials is any substance whose dimensions fall between 1–100 nm. Their high surface area to volume ratio, capacity to create protective layers and oxidation resistance are just a few features that make them ideal for corrosion prevention. Using nanomaterials, which have shown extraordinary characteristics and unique behaviours owing to their nanoscale size, provides a

*Corresponding author. E-mail: sunil0520@gmail.com

viable route in this endeavour [4]. Co_3O_4 nanoparticles are one type of nanomaterial that has shown promise for corrosion protection. Co_3O_4 is a transition metal oxide with several properties that make it well-suited for this application. It is an excellent electrical conductor, can form a protective layer on the material's surface, and is oxidation-resistant. The exceptional physicochemical features and exhibited effectiveness in various applications make cobalt oxide (Co_3O_4) nanoparticles a desirable contender among these nanomaterials. In particular, they are desirable candidates for enhancing the durability and lifetime of electrode materials in electrochemical devices due to their resistance to corrosion under severe operational conditions [5]. The temperature-dependent properties of Co_3O_4 nanoparticles in anticorrosive applications play a critical role in determining their effectiveness and stability under varying environmental conditions. The ambient temperature has an important role in determining the corrosion resistance of electrode materials. Anticorrosive behaviour may be affected by changes in temperature because of the electrochemical reactions at the electrolyte-electrode interface. For this reason, studying the anticorrosive characteristics of Co_3O_4 nanoparticles as a function of temperature is crucial to understanding their potential as a dependable protective layer for electrode materials [6]. Zinc is a naturally corrosion-resistant metal, so a zinc plate can be used to protect other metals from corrosion. Cobalt oxide (Co_3O_4) coated on a zinc plate in a KOH electrolyte can be used to improve the anti-corrosion properties of the zinc plate. In KOH electrolyte, Co_3O_4 can form a protecting layer on the zinc plate's surface that helps prevent the zinc from corroding. This layer is formed by electrochemical oxidation, in which the Co_3O_4 nanoparticles react with the KOH electrolyte to form a protective film. They provide improved anti-corrosion properties and a stable, protective layer and are effective in various applications [7].

In this study, we use nanotechnology and electrochemistry to understand better the complex relationship between Co_3O_4 nanoparticles and temperature regarding corrosion protection. We use a simple sonochemical approach to understand further how Co_3O_4 nanoparticles' anticorrosive capabilities change with temperature (400, 500 and 600 °C). Here, the optical and physico-chemical properties of the synthesized Co_3O_4 nanoparticles have been scrutinized. Further, the electrochemical impedance spectroscopy (EIS) and linear sweep voltammetry (LSV) studies have been analyzed and evaluated. The impact of Co_3O_4 nanoparticles on the corrosion inhibition performance of zinc plates in KOH electrolytes was discussed.

EXPERIMENTAL

Chemicals

Cobalt nitrate hexahydrate ($Co(NO_3)_2.6H_2O$), ammonia solution ($NH_3.OH$), zinc plate, potassium hydroxide (KOH), pH paper and double-distilled water (DD) were all analytical-grade reagents procured from Merck and utilized (99.9% pure) without additional distillation processes.

Synthesis of Co_3O_4 nanoparticles

For a homogenous solution, 0.1 M cobalt nitrate hexahydrate was immersed in 100 mL distilled water and agitated for 20 min at a constant rpm. Then 100 mL of an ammonia solution was mixed and added slowly to the cobalt nitrate solution unless the pH reached 12. The solution was then subjected to ultrasonication. The solution was sonicated at a frequency of 40 Hz for 60 min. The resultant solution was dried out in the 80 °C hot-air oven overnight. The fine powder was then calcined for three hours at 400 °C in a muffle furnace to evacuate loosely attached atoms and ions, including residual nitrate. Figure 1 depicts the graphical illustrations of the Co_3O_4 nanoparticle synthesis process.

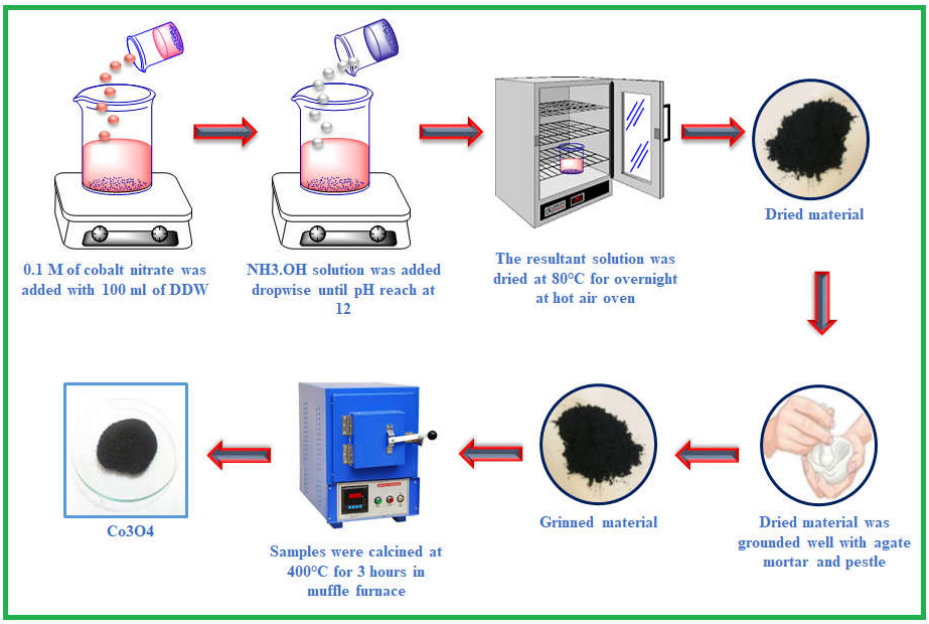

Figure 1. Schematic representation of Co_3O_4 nanoparticles synthesis.

Electrochemical preparation and performances

A single-step coating technique with an aqueous solution and no electrical current is suitable for preparation and environmental impact. The zinc metal plate was utilized to evaluate Co_3O_4's anticorrosive properties. After cleaning with acetone and deionized water, the Zn metal plate was dried in a hot-air oven after being polished with 9 mm, 3 mm, and 1 mm SiC grit papers. A slurry was made by mixing 15 mg of Co_3O_4 with 80:15:5 weight ratios of polyvinylidene difluoride and N-methyl-2-pyrrolidone. The doctor's blade method was used to coat the slurry on top of a 1 cm^2 area on the surface of the zinc metal plate [6, 7]. The coating was performed thrice to get a homogeneous layer of Co_3O_4 nanoparticles on the metal surface. The coated plate was dried in a hot-air oven at 353 K for an hour and utilized for corrosion tests in a 6 M KOH electrolyte atmosphere. For the temperature-dependent corrosion evaluation, the coated plates are annealed at 400, 500 and 600 °C for two hours at the muffle furnace. The elemental details of the Zn plate used in this study are given in Figure 2.

Characterization techniques

The structural pattern of the created Co_3O_4 NPs was determined via a X-ray diffractometer (X'Pert PRO; Almelo, the Netherlands). By an FTIR spectrophotometer (Spectrum 100; PerkinElmer, USA), we could record the IR (400-4,000 cm^{-1}) spectra of Co_3O_4 NPs. The average particle size distribution was calculated using the dynamic light scattering (DLS) technique and a 633 nm laser light source with a particle size analyzer (Nanophox; Sympatec, Germany). After 24 hours in KOH electrolytes, the corrosion-inhibiting effects of Co_3O_4 coatings on Zn plates were investigated. At room temperature, the Zn/Co_3O_4 plates' electrochemical corrosion behavior was investigated utilizing a three-electrode setup and an electrochemical workstation (PGSTAT302N;

Metrohm Autolab, the Netherlands). All of the coated samples were characterized for their topographical properties, roughness, and hardness using an in-situ scanning probe microscope (SPM) with a Berkovich nanoindenter and quasistatic software before and after electrolyte immersion and linear sweep voltammetry (LSV) testing. The prepared specimen (10 m area) was loaded to its maximum of 600 N for 15 s when the force was applied and removed at 100 N/s. Microstructure analysis was also used to investigate the coating's roughness. Uncoated metal plates were evaluated by measuring their surface characteristics.

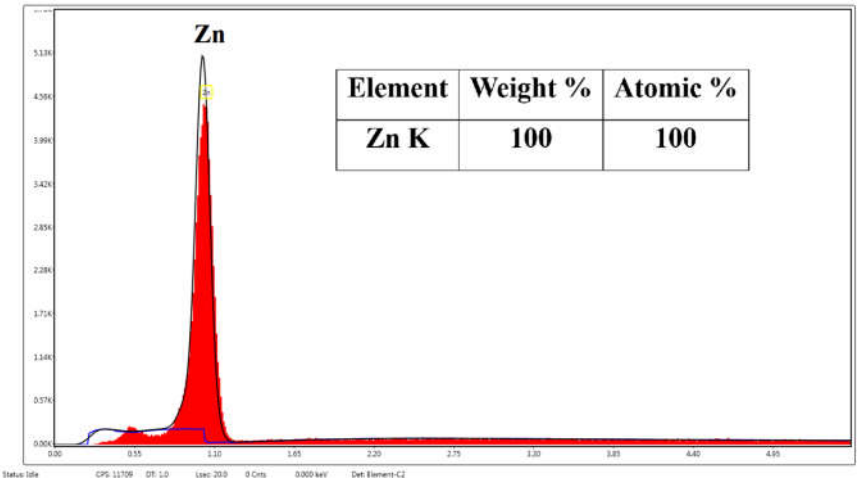

Figure 2. Elemental composition analysis of Zn metal plate.

RESULTS AND DISCUSSION

X-Ray diffraction analysis

Figure 3 illustrates the synthesized XRD patterns of cobalt oxide (Co_3O_4) nanoparticles. Crystal planes (200), (311), (222), (400), (422), (511), (440), (620), and (533) correspond to the diffraction peaks noticed at (31.272°), (38.542°), (44.810°), (59.350°), (65.238°), (74.221°), and (78.40°). Each of the diffraction peaks lined up perfectly with the face-centered cubic (FCC) crystalline phase of Co_3O_4 NPs (a=b=c=8.083 and α=β=γ=90°) in the crystallographic space group Fd3m (227). No extra peaks equivalent to other phases of cobalt oxide, such as cobalt monoxide and cobalt hydroxide were observed, and the presence of a maximum intensity peak at 36.853° (311) indicated the purity of single-phase and polycrystalline nature of the synthesized materials [9, 10]. The lack of additional peaks in the diffraction patterns indicates the sample's phase purity. This is because the absence of other peaks indicates that distinct phases, such as CoO and CO_2O_3, are absent. The following relations determined the unit cell volume *V*, lattice parameter α, and the synthesised FCC structures' average crystallite size (D) [11]:

$$\frac{1}{d^2} = \frac{h^2+k^2+l^2}{a^2} \quad (1)$$

Interplanar distance (d), Miller indices (h, k, l), and lattice constant (a) comprise every parameter in this equation.

$$V = a^3 \quad (2)$$

where, lattice constant *a* multiplied by the volume of a unit cell *V*.

$$D = \frac{k\lambda}{\beta cos\theta} \quad (3)$$

where D is the average crystallite size, which was determined by taking measurements from three significant predominant peaks; *k* is the shape factor, which is equal to 0.9; is λ the wavelength of the X-ray source (1.5406 Å); β is the FWHM of all diffraction peaks; and Θ is the Bragg's diffraction angle. The simple preparation procedures are essential for stabilizing the Co_3O_4 nanoparticles and preventing them from agglomeration. The ammonia solution transfers electrons from the functional group of the donors to the transition metal elements, which are also capable of creating coordination compounds. As a result, the unique source precursor of the Co $(OH)_2$ complex form is decomposed, which leads to the formation of Co_3O_4 nanoparticles. This process is accomplished by reducing complex forms of cobalt ions to cobalt ions with the charge of Co^{2+}. Full Proof analytical program is utilized to perform Rietveld refinement on XRD patterns for qualitative analysis (Figure 3). The Pseudo-Voigt function is used to further enhance XRD patterns against a constant background. Co_3O_4 NPs refinement data yields the space group Fd3m (227) with a cubic structure and a lattice parameter of a=b=c=8.085 Å. Previous results are in excellent agreement with the refining parameters [24-26].

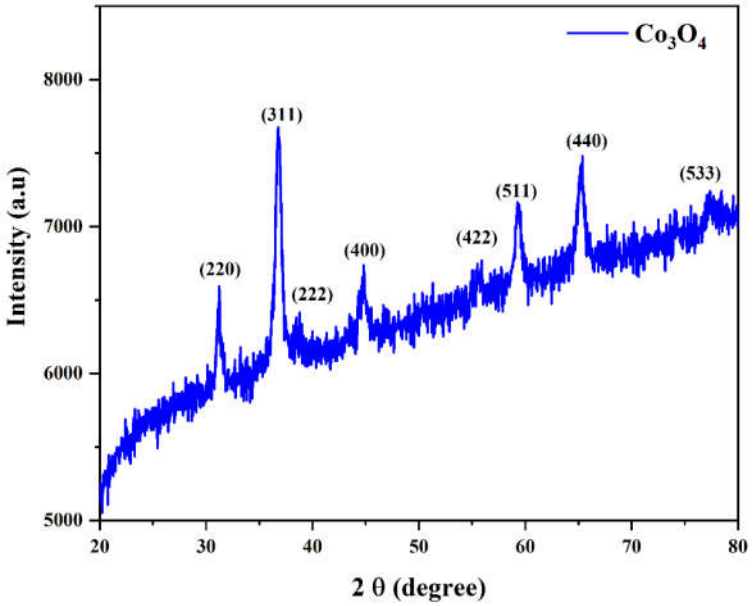

Figure 3. XRD pattern of Co_3O_4 nanoparticles.

Electrochemical corrosion studies

The electrochemical corrosion behavior of bare and Co_3O_4 NPs-coated zinc plates was analyzed by linear-sweep voltammetry (LSV) under an aqueous electrolyte medium, 6 M KOH. Figure 4 (a, c, and e) shows the LSV curve, and Figure 4 (b, d, and f) shows the Tafel plot or potentiodynamic polarization curve for uncoated and Co_3O_4 coated Zn plates in the aqueous electrolyte solution. The role of temperature on the anticorrosion performance of the prepared Co_3O_4 nanoparticles is evaluated by thermally treating the coated plates. The coated plates are

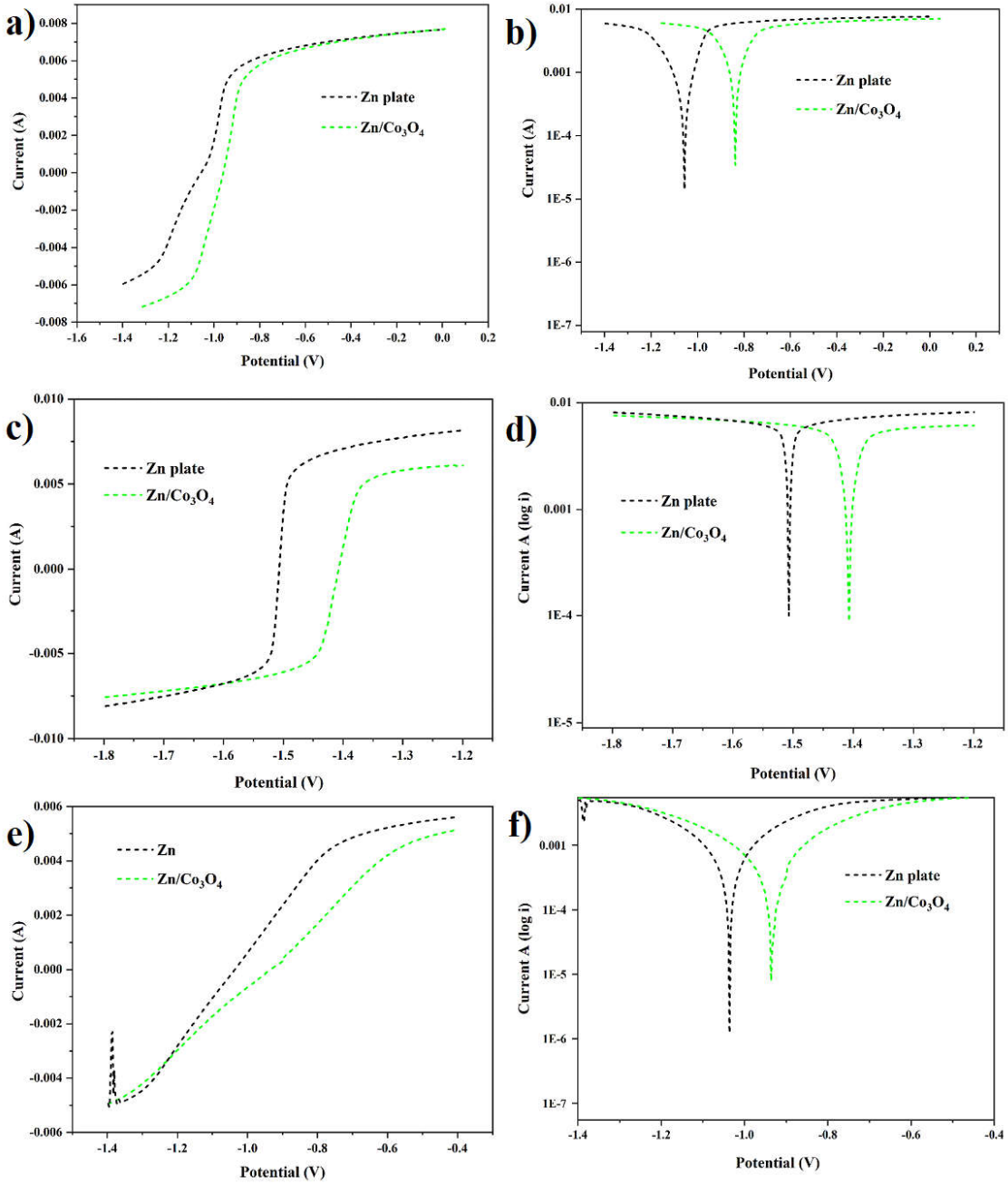

Figure 4. LSV curves (a, c, and d) and Tafel plot (b, d and f) of Co_3O_4 nanoparticles.

thermally treated for 400, 500 and 600 °C. On initial application of −1.4 V potential, Zn plates start corroding at the anode. The potential has a tendency to reach −0.4 V with an interval of ~5 mV. From the Tafel plot, it is apparent that the corrosion potential of both plates is moved to the positive region. The decrease in the corrosion current and corrosion rate of Co_3O_4 nanoparticles coated Zn plate increased the polarization resistance, which could be as a result of the thin layer coating on cobalt oxide on the surface of the zinc anode [12]. Interestingly, the Zn/Co_3O_4 plate showed more than twice the improved corrosion resistance of about 78.44% for 400 °C treated Zn plate samples. The corrosion curves of 500 °C treated Zn plates in the presence of 6 M KOH electrolyte medium are depicted in Figure 5 (c and d), which reveal the corrosion potential of both samples moving toward the positive side compared to the bare Zn plate. In this case, the corrosion resistance percentage of the Zn/Co_3O_4 plate was higher than that of bare Zn, with increased polarization resistance and decreased corrosion current and corrosion rate. These obtained values are given in Table 1. The potentiodynamic polarization curve of bare Zn, Zn/Co_3O_4 plates at 600 °C treated samples is shown in Figure 4 e and f. This plot reveals that the Zn/Co_3O_4 plate has lower corrosion current and corrosion rate than the Zn plates, which could be ranged in increasing order: Zn/Co_3O_4 < Zn, which leads to improved corrosion resistance. While increasing the annealing temperature of the coated plates, the grains gradually merge with each other's and their sizes increase progressively. These grain size changes will help form a strong layer of Co_3O_4 nanoparticles on the Zn plate surface [13-15].

The Tafel plot shows a decrease in the current density value for the Co_3O_4 NPs-coated Zn plates compared to that for the base plates (Zn). This suggested an improvement in the polarization resistance behavior, which could be attributed to the microstructural variation and intrinsic features of the Co_3O_4 NPs. The corrosion current (I_{corr}) and E_{corr} values for the cathodic and anodic regions of Tafel plot are shown in Table 1. The typical corrosion rates of the pure and Co_3O_4 nanoparticles coated Zn plates were compared. It was noticed that the corrosion rate of the synthesized Co_3O_4 NPs-coated, compared to the pure Zn plates, decreases by about 43.7% owing to the reduction in defects and particle clusters. In addition, an increased number of refined grains in the Co_3O_4 NPs-coated Zn plate enhanced the development of the passive film on the surface, which protected the Zn plate against corrosion [16]. The results of Co_3O_4 nanoparticles coated Zn plates showed that Co_3O_4 NPs-coated Zn plates exhibited a lower corrosion rate of about 45.8% than pure Zn plates. This could be because the electrochemical reaction between Co and O ions is higher in the KOH electrolytes than in the pure Zn plate. This indicates that the Zn plate does not interact with K ions; hence, the Co_3O_4 NPs-coated Zn plate maintains a passivation layer.

Table 1. Parameters of Tafel polarization for bare and Co_3O_4 NP-coated Zn plates in KOH electrolyte.

Temp. °C	Sample	Ecorr (V)	Icorr (μA/cm^2)	Polarization resistance (Ω)	Corrosion rate (mm/yr)	Improved corrosion resistance (%)
400	Zn plate	-1.508	955.1	2.999	14.36	-
	Zn/Co_3O_4	-1.407	856.2	8.199	6.509	54.66
500	Zn plate	-1.180	236.4	187.3	2.747	-
	Zn/Co_3O_4	-1.036	98.31	75.13	0.789	71.24
600	Zn plate	-1.0274	420.4	38.91	4.885	-
	Zn/Co_3O_4	-1.1487	176.7	72.53	1.053	78.44

Co_3O_4 nanoparticle coatings created in the present study showed significant improvements in corrosion resistance compared to pure Zn plates, supporting the assumptions made in the preceding discussion and the provided experimental findings. On the other hand, temperature treatment of the coated plates played a vital role in anti-corrosion performance. The plate's annealing temperature impacts corrosion resistance in the following order: 400 °C < 500 °C < 600 °C. The measured corrosion resistance values of the Co_3O_4-coated MS plates are compared with

earlier reports of metal oxides on various metal subtracts. The comparative assessment is given in Table 2.

Table 2. Nanomaterial coatings on metal surfaces for improved corrosion resistance: a comparative study.

S. No.	Inhibitor	Substrate	Electrolyte	Corrosion resistance efficiency (%)	Ref
1	ZnO	MS	3.5% NaCl	50.1	36
2	CuO	MS	3.5% NaCl	53.57	37
3	Mn_2O_3	MS	1 M HCl	72.63	38
4	CdS	Zn	1 M HCl	70.09	39
5	ZnS	MS	1 M HCl	73.65	40
6	NiO-Zn	MS	3.5% NaCl	49.7	41
7	Ni-Zn-Epoxy	Steel	3.5% NaCl	75.4	42
8	ZrO2	316L SS	1 M H_2SO_4	69.1	43
9	Co_3O_4	Zn	6 M KOH	78.44	This work

Contact angle and Vickers hardness measurement

The electrochemical measurements were performed under aqueous conditions, so the contact angle should be critical to electrode and electrolyte interaction. The surface contact angle for the bare Zn plate is 70°, consistent with the earlier reports [17]. When Co_3O_4 nanoparticles are coated on the surface of the Zn plate, the contact angle of the Zn plate is 96°, 112° and 137°, respectively, for annealed samples at 400, 500 and 600 °C which indicates that the surface of the Zn plate changed to more hydrophobic nature. The role of annealing temperature on the coated plates' microhardness is measured by Vickers hardness testing (ASTM E384) equipment. Hardness analysis is repeated four times at four different places on the surface of the Co_3O_4 nanoparticles-coated Zn plates. As observed in these results, the microhardness of the bare Zn plate is 117 HV, and 400, 500 and 600 °C coated plates are enhanced linearly, i.e., 151 HV, 177 HV, and 197 HV after heat treatment. After annealing the coatings, an inverse Hall-Petch effect is observed, i.e., the coatings become harder as the particle size increases by increasing the annealing temperature to 600 °C. Figure 5 represents the surface of the plates (optical microscopic images). The characteristics of the microhardness findings are comparable to those of previous studies. Recrystallization occurs on the surface during the tempering phases, reducing the dislocation density. Therefore, the formed dislocations move more efficiently during indentation, resulting in a modest reduction in surface hardness [18].

Surface analysis of Co_3O_4 nanoparticles coated Zn plates

The surfaces of the electrode materials are typically wherein electrochemical reactions are initiated and carried out. The electrochemical corrosion processes may be affected by the surface characteristics [14, 15]. The elimination of surface roughness is one way to protect against electrochemical corrosion. Correspondingly, scanning probe microscopy (SPM) was used to scrutinize uncoated Zn, and Co_3O_4 nanoparticles coated Zn plates. Figures 6 and 7 provide topographical photographs of bare Zn, Co_3O_4 nanoparticles coated Zn plates in two dimensions (2D) and three dimensions (3D), respectively, before and after the electrochemical reactions. The 2D and 3D photographs demonstrate normal grain sizes with uneven, heterogeneous peaks before and after corrosion of bare and Co_3O_4 coated Zinc plates after annealing at 400, 500 and 600 °C.

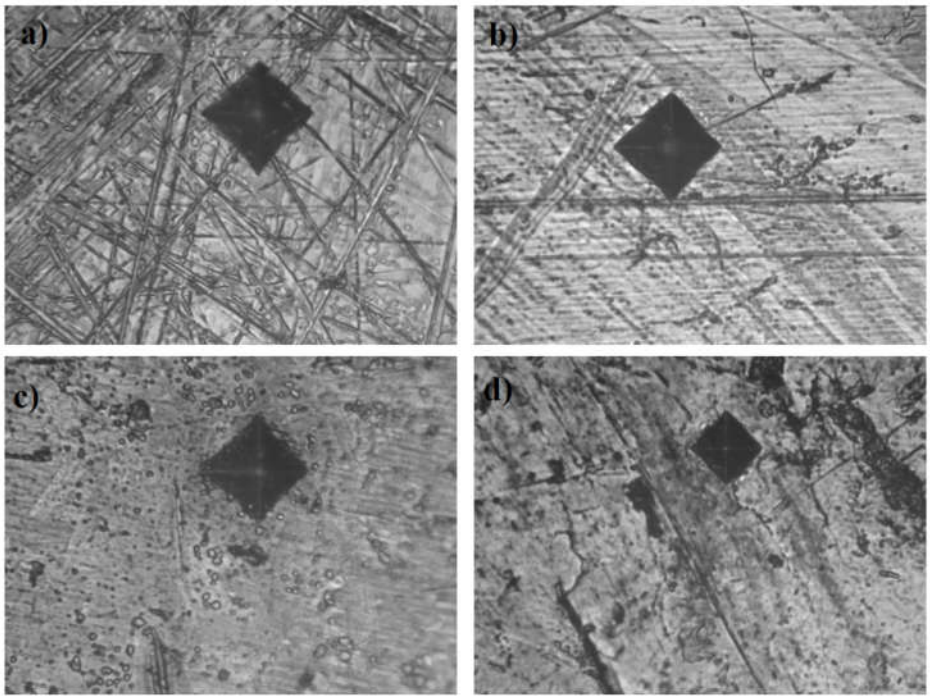

Figure 5. Optical microscopic images of Co_3O_4 nanoparticles coated plates annealed at different temperature.

The surface roughness was consistently enhanced when electrochemical reactions occurred compared to each sample. Table 3 presents the microstructural features of the bare and Co_3O_4 coated Zn plates after annealing at 400, 500 and 600 °C, which were analyzed using in-situ scanning probe microscopy before and after the electrochemical processes [19]. The extent to which corrosion may be inhibited is inversely related to the plate's depth displacement.

Table 3. Microstructure surface properties of bare and Co_3O_4 coated zinc plates under KOH electrolyte.

Sample	Maximum depth displacement (h) nm	Average surface roughness (Ra) nm	
		Before corrosion	After corrosion
Zn plate	1544	83.051	131.58
Zn/Co_3O_4-400	1365	45.53	96.55
Zn/Co_3O_4-500	988	46.17	83.05
Zn/Co_3O_4-600	917	43.55	71.09

The coated MS plate's surface roughness values increased after electrochemical analysis. Surface roughness values increase due to interactions between hydrogen and chlorine ions and the Co_3O_4 nanoparticle coating. Despite this, the Zn plate did not have its surface refinished with the Co_3O_4 coating. The electrochemical investigation found that the roughness of the zinc plate's surface had significantly increased [20-22]. Bare and Co_3O_4-coated Zn plates would both exhibit an increase in surface roughness due to the electrochemical reaction. The type of adhesion heavily influences the endurance of the nanoparticle coating on metal surfaces. The electrochemical procedure has less than a 15% impact on the coated area, durability and suggests high adherence to the Zn plate surface as revealed in Figure 7.

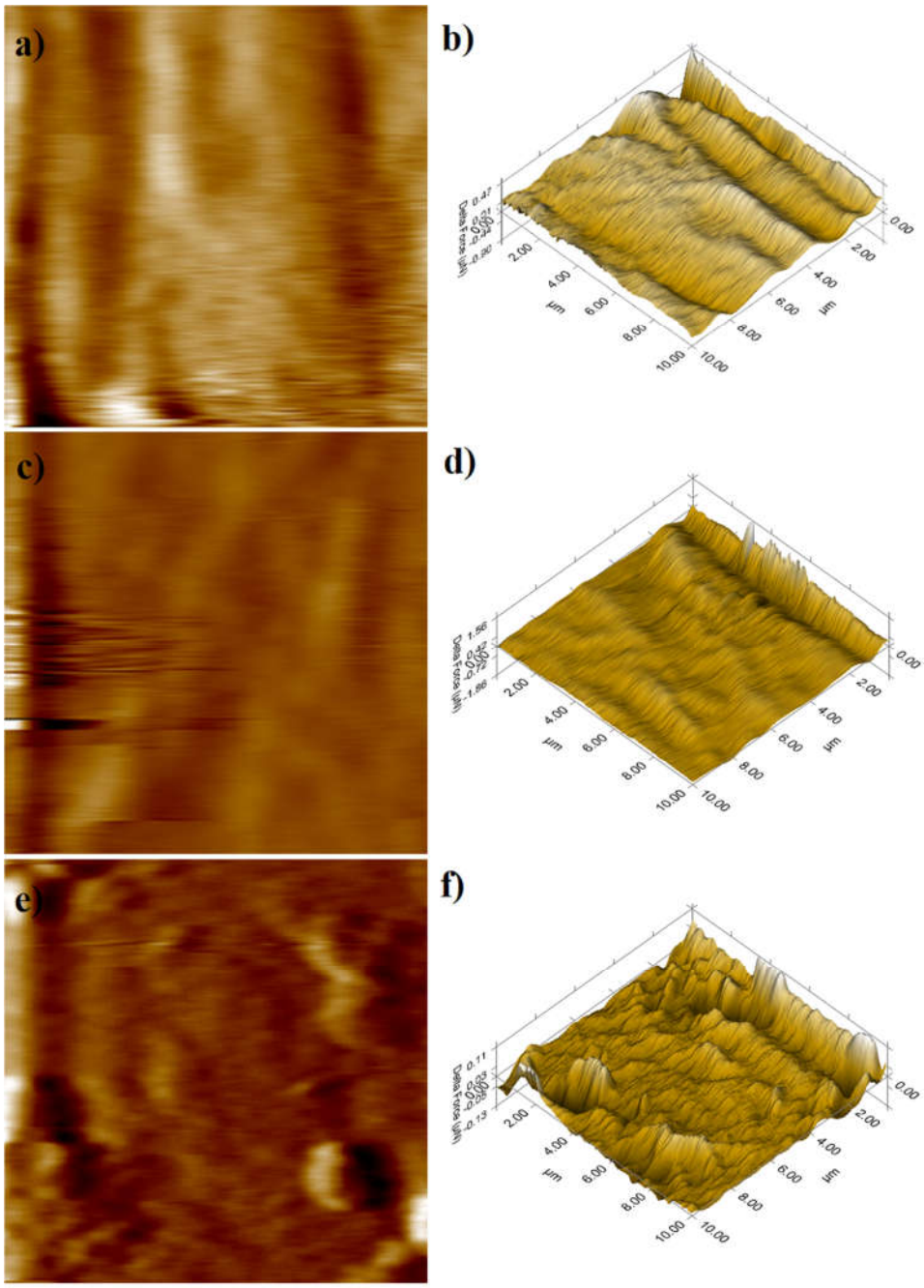

Figure 6. In-situ SPM analysis of bare and Co_3O_4 coated zinc plates before electrochemical reactions.

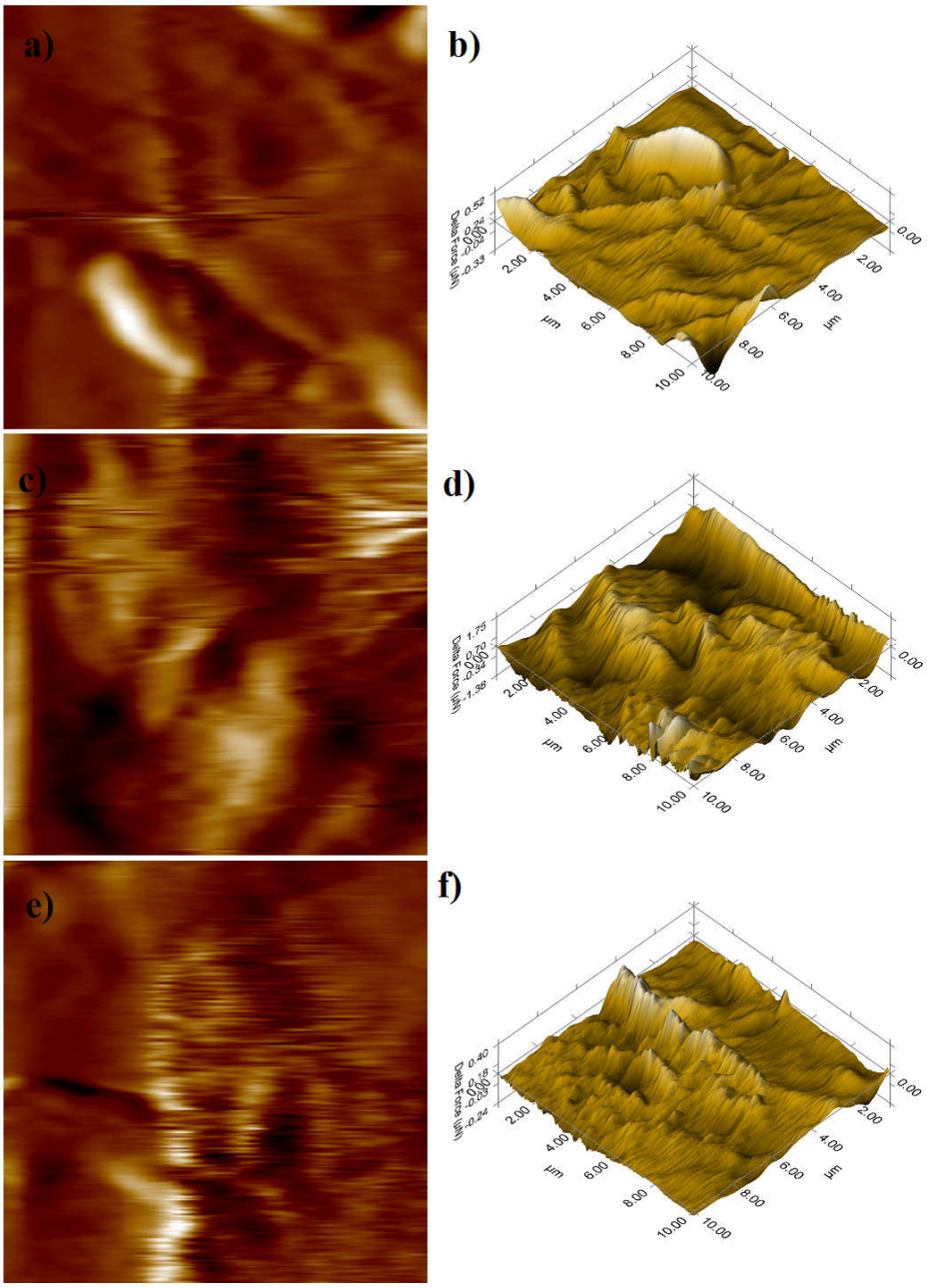

Figure 7. In-situ SPM analysis of bare and Co_3O_4 coated zinc plates after electrochemical reactions under KOH electrolyte.

CONCLUSION

A super-hydrophobic surface was fabricated on a zinc metal plate substrate via the doctor's blade coating procedure for synthesis of cobalt oxide nanoparticles, which is a simple, one-step, environmentally benign approach. Cubic structure with the creation of a low surface energy spherical-like structure of cobalt oxide nanoparticles has been confirmed via X-ray diffraction, FTIR and SEM analysis. It was found that the annealing temperature impacted not only the physical morphology of the surface but also its composition and wetting characteristics. The temperature-dependent electrochemical corrosion resistance behaviors were evaluated using linear sweep voltammetry analysis. Co_3O_4 nanoparticles obtained the optimum super-hydrophobic surface-coated Zn plates by annealing at 600 °C for one hour, with a maximum contact angle of 142 and a most significant rate of corrosion resistance value of about 78.44%. The SPM analysis revealed the physical stability of the coatings even after the electrochemical reactions. The high-temperature treated samples show a minimum change in surface roughness values (about 71.09 nm). In addition, it is anticipated that such a technique might provide a novel method for increasing the applications and durability of Zn metal plates as electrodes in energy storage applications.

REFERENCES

1. Jiang, S.P. Development of lanthanum strontium cobalt ferrite perovskite electrodes of solid oxide fuel cells-A review. *Int. J. Hydrogen Energy* **2019**, 44, 7448–7493.
2. Olivo, A.; Beyribey, B.; Kim, H.; Persky, J. Cobalt oxide enhanced lanthanum strontium cobalt ferrite electrode for solid oxide fuel cells. *Main Group Chem.* **2022**, 21, 195–207.
3. Ishii, A.; Nemoto, N.; Yamaguchi, M.; Kobayashi, K.; Oikawa, I.; Takano, A.; Hitomi, T.; Hayashi, N.; Takamura, H. Key role of interfacial cobalt segregation in stable low-resistance composite oxygen-reducing electrodes. *ACS Appl. Mater. Interfaces* **2023**, 15, 34809–34817.
4. Kavitha, V.; Mayandi, J.; Mahalingam, P.; Sethupathi, N. Structural, optical and electrical studies on zinc doped barium strontium titanate as photo-anode for DSSC device. *Mater. Today: Proc.* **2021**, 35, 48–52.
5. Alaboodi, A.S.; Hussain, Z. Finite element modelling of nanoindentation technique to characterize thin film coatings. *J. King Saud Univ. Eng. Sci.* **2019**, 31, 61–69.
6. Kandalkar, S.G.; Lee, H.M.; Chae, H.; Kim, C.K. Structural, morphological, and electrical characteristics of the electrodeposited cobalt oxide electrode for supercapacitor applications. *Mater. Res. Bull.* **2011**, 46, 48–51.
7. Banu, A.; Marcu, M.; Alexandrescu, E.; Anghel, E.M. Electrochemical deposition and characterization of polypyrrole coatings doped with nickel cobalt oxide for environmental applications. *J. Solid State Electrochem.* **2014**, 18, 2661–2671.
8. Gupta, P.; Kumar, D.; Quraishi, M.A.; Parkash, O. Effect of cobalt oxide doping on the corrosion behavior of iron-alumina metal matrix nanocomposites. *Adv. Sci. Eng. Med.* **2013**, 5, 1279–1291.
9. Kandalkar, S.G.; Gunjakar, J.L.; Lokhande, C.D. Preparation of cobalt oxide thin films and its use in supercapacitor application. *Appl. Surf. Sci.* **2008**, 254, 5540–5544.
10. Chang, J.K.; Lee, M.T.; Huang, C.H.; Tsai, W.T. Physicochemical properties and electrochemical behaviour of binary manganese–cobalt oxide electrodes for supercapacitor applications. *Mater. Chem. Phys.* **2008**, 108, 124–131.
11. Jafari, A.; Alam, M.H.; Dastan, D.; Ziakhodadadian, S.; Shi, Z.; Garmestani, H.; Weidenbach, A.S.; Ţalu, S. Statistical, morphological, and corrosion behaviour of PECVD derived cobalt oxide thin films. *J. Mater. Sci.: Mater. Electron.* **2019**, 30, 21185–21198.
12. Priyan, S.R.; Kumar, G.S.; Surendhiran, S.; Shkir, M. Size-controlled synthesis of mesoporous silica nanoparticles using rice husk by microwave-assistedsol–gel method. *Int. J. Appl. Ceram. Technol.* **2023**, 20, 2807–2816.

13. Karthikeyan, S.; Dhanakodi, K.; Shanmugasundaram, K.; Surendhiran, S. Synthesis and characterization of lanthanum oxide nanoparticles: A study on the effects of surfactants. *Mater. Today: Proc.* **2021**, 47, 901–906.
14. Patterson, A.L. The Scherrer formula for X-ray particle size determination. *Phys. Rev.* **1939**, 56, 978–982.
15. Vasudevan, D.; Senthilkumar, D.; Surendhiran, S. Performance and characterization studies of reduced graphene oxides aqua nanofluids for a pool boiling surface. *Int. J. Thermophys.* **2020**, 41, 74–81.
16. Shaju, K.M.; Guerlou-Demourgues, L.; Godillot, G.; Weill, F.; Delmas, C.; Strategies for synthesizing conductive spinel cobalt oxide nanoparticles for energy storage applications. *J. Electrochem. Soc.* **2012**, 159, A1934.
17. Mei, J.; Liao, T.; Ayoko, G.A. Cobalt oxide-based nano architectures for electrochemical energy applications. *Prog. Mater Sci.* **2016**, 103, 596–677.
18. Prabaharan, D.D.M.; Sadaiyandi, K.; Mahendran, M.; Sagadevan, S. Precipitation method and characterization of cobalt oxide nanoparticles. *Appl. Phys. A: Mater. Sci. Process.* **2017**, 123, 264–272.
19. Rahimi, M.; Naderi, H.R.; Karimi, M.S.; Ahmadi, F.; Pourmortazavi, S.M. Cobalt carbonate and cobalt oxide nanoparticles synthesis, characterization and supercapacitive evaluation, *J. Mater. Sci.: Mater. Electron.* **2017**, 28, 1877–1888.
20. Salavati, M.; Khansari, A.; Davar, F. Synthesis and characterization of cobalt oxide nanoparticles by the thermal treatment process. *Inorg. Chim. Acta* **2009**, 362, 4937–4942.
21. Iravani, S.; Varma, R.S. Sustainable synthesis of cobalt and cobalt oxide nanoparticles and their catalytic and biomedical applications. *Green Chem.* **2020**, 22, 2643–2661.
22. Deepa, K.; Venkatesha, T.V. Comparative anti-corrosion performance of electrochemically produced Zn–NiO and Zn–NiO–ZrO_2 composite coatings on mild steel. *Surf. Eng. Appl. Electrochem.* **2019**, 55, 317–323.